Thermochimica Acta 511 (2010) 152–158

Contents lists available at ScienceDirect

Thermochimica Acta

journal homepage: www.elsevier.com/locate/tca

Crystallization and melting behavior of β-nucleated isotactic polypropylene/polyamide 6 blends with maleic anhydride grafted polyethylene-vinyl acetate as a compatibilizer

Zhugen Yang[a,b], Kancheng Mai[a,*]

[a] Materials Science Institute, School of Chemistry and Chemical Engineering, Sun Yat-Sen University, Key Laboratory of Polymeric Composites and Functional Materials of the Ministry of Education, Guangzhou 510275, PR China
[b] Institut des Nanotechnologies de Lyon, UMR 5270 CNRS, École centrale de Lyon, Equipe Chimie et Nanobiotechnologies, 36 Avenue Guy-de-Collongue, 69134 Ecully, France

ARTICLE INFO

Article history:
Received 1 June 2010
Received in revised form 19 July 2010
Accepted 6 August 2010
Available online 13 August 2010

Keywords:
β-Crystal
iPP/PA6 blend
EVA-g-MA
Crystallization behavior
Melting characteristic

ABSTRACT

β-Nucleated isotactic polypropylene (β-iPP) blend with maleic anhydride grafted polyethylene-vinyl acetate (EVA-g-MA) and β-iPP/polyamide (PA) 6 blend, as well as its compatibilized version with EVA-g-MA as a compatibilizer were prepared with an internal mixer. Analysis from differential scanning calorimeter (DSC) and wide angle X-ray diffraction (WAXD) indicates that the addition of EVA-g-MA into β-nucleated iPP decreases the crystallization temperature (T_c^p) of PP, but it has no pronounced influence on the β-crystal content for β-nucleated iPP. For β-nucleated iPP/PA6 blends, PA6 obviously decreases the β-crystal content. However, the addition of EVA-g-MA is quite benefit for the formation of β-crystal in β-nucleated iPP/PA6 blends and the β-crystal content increases with increasing EVA-g-MA content. It is suggested that the nucleating agent mainly disperses in the PA6 phase and/or the interface between iPP and PA6 in iPP/PA6 blend, which was proved by etching the blends with sulfuric acid and experimental facts from SEM.

1. Introduction

Isotactic polypropylene (iPP) is one of the most versatile commodity thermoplastic polymers because it possesses exceptional properties including excellent chemical and moisture resistance, good ductility and low manufacturing cost. What's more, iPP is a polymorphic material with three known possible crystal forms, namely, monoclinic (α-crystal), trigonal (β-crystal), and triclinic (γ-crystal) [1,2]. Recently, more attentions are focused on the β-crystal owning to its excellent thermal and mechanical properties, such as higher thermal deformation temperature, improved elongation at break and impact strength, which are very important from the viewpoint of industrial application [2–8]. However, due to its lower stability in comparison with the α-iPP, high content of β-crystal can only be obtained under special crystallization conditions such as the introduction of a β-nucleating agent [9–13], a temperature gradient [14–16] and shearing or elongation of the melt [17–20]. Moreover, the yield strength and elastic modulus of β-iPP are lower than those of α-iPP. In order to improve the properties of β-iPP, β-iPP blending with other polymers shall be become an increasingly important method.

Feng et al. [21] observed that the shear flow field during cavity filling significantly influenced the formation of β-crystal in the blends of iPP and polyamide 6/clay nanocomposites (iPP/NPA6). The high shear between the NPA6 phase and the iPP matrix can induce the formation of β-crystal under proper crystallization conditions in the mold. They also found that the introduction of NPA6 rather than PA6 in blends with iPP induced significant β-iPP during injection molding. However, the formation mechanism involved in the process is needed to further understand. It has been observed that β-iPP blends can be prepared without any difficulty if compounded with amorphous, e.g., elastomer [22,23] and one of the important factors of the formation a blend with β-iPP is the α-nucleation effect of the second component [24–28]. If the crystallization temperature (T_c^p) of the second component with α-nucleating effect is lower than that of iPP, it has little effect on the formation of β-iPP. On the contrary, if the T_c^p of the second component with α-nucleating effect is higher than that of iPP, it suppresses the formation of β-iPP, e.g., in the β-nucleated iPP/poly(vinylidene-fluoride) (PVDF) and iPP/polyamide 6 (PA6) blends, the β-iPP cannot form even in the presence of a highly effective β-nucleating agent due to the strong α-nucleating ability and higher T_c^p of PVDF and PA6.

According to our previous work [26–28], the content of β-crystal decreases with increasing the PA6 content for β-nucleated iPP/PA6 blends, but high content of β-crystal can be obtained in the β-

* Corresponding author. Tel.: +86 20 84115109; fax: +86 20 84115109.
E-mail address: cesmkc@mail.sysu.edu.cn (K. Mai).

0040-6031/$ – see front matter © 2010 Elsevier B.V. All rights reserved.
doi:10.1016/j.tca.2010.08.007

Table 1
DSC data of iPP component in β-iPP/EVA-g-MA and β-iPP/PA6 80/20 blends compatibilized with EVA-g-MA[a].

Samples	Crystallization			Melting				
	T_c^{on} (°C)	T_c^{p} (°C)	$-\Delta H_c$ (J/g)	T_m^{p} (°C)			ΔH_m (J/g)	K_β (%)
				β1	β2	α		
β-iPP/EVA-g-MA								
100/0	126.4	124.3	87.4	–	150.7	163.1	85.1	97
95/5	121.8	124.3	80.7	149.5	153.7	162.1	84.2	98
90/10	118.2	121.0	81.7	147.2	153.8	160.7	88.3	96
85/15	117.2	119.8	84.2	146.5	153.7	160.3	83.9	96
80/20	119.4	116.3	85.8	146.6	153.9	160.9	87.8	97
80/20/0	125.0	123.1	91.8	149.5	–	162.4	90.6	66
β-iPP/PA6/EVA-g-MA								
80/20/2	124.0	121.6	85.9	148.7	153.6	161.7	88.9	80
80/20/5	122.1	119.5	89.0	147.6	153.7	161.0	90.8	89
80/20/8	121.1	118.5	89.5	146.9	153.7	160.5	90.0	91
80/20/10	120.4	117.8	93.9	146.9	153.8	160.5	91.2	96

[a] T_c^{on}, onset temperature of crystallization; T_c^{p}, temperature of crystallization peak; ΔH_c, enthalpy of crystallization, T_m^{p}, temperature of melting peak; ΔH_m, enthalpy of fusion, K_β, the relative percentage of β-phase calculated according to WAXD; the unit of each composition for β-iPP/PA6/EVA-g-MA is phr.

nucleated iPP/PA6 compatibilized with maleic anhydride grafted PP (PP-g-MA) and it is not obviously influenced by the PA6 content. Menyhárd et al. [24,29] also observed that the formation of α-iPP matrix in β-nucleated iPP/PA6 without a compatibilizer is related to the selective encapsulation of β-nucleating agent in the polar PA6 phase but the addition of PP-g-MA can improved the distribution of β-nucleating agent in iPP phase to form a matrix rich in β-crystal. However, this explanation is needed to be proved by further experimental facts. Moreover, the distribution of nucleating agents in the different phases is still an open question in general and there is still no report about how the compatibilizer improved the formation of β-crystal in the β-nucleated iPP/PA6 blends except PP-g-MA. As a consequence, the main goal of this study was to find out the effect of EVA-g-MA, as a compatibilizer, on the crystallization behavior, melting characteristic and β-crystal content of the iPP/PA6 blends. Additionally, we try to prove the hypothesis that the nucleating agents mainly disperse in the PA6 phase and/or the interface between iPP and PA6 in the process of mixing at high temperature by etching the blends with sulfuric acid and SEM experimental facts.

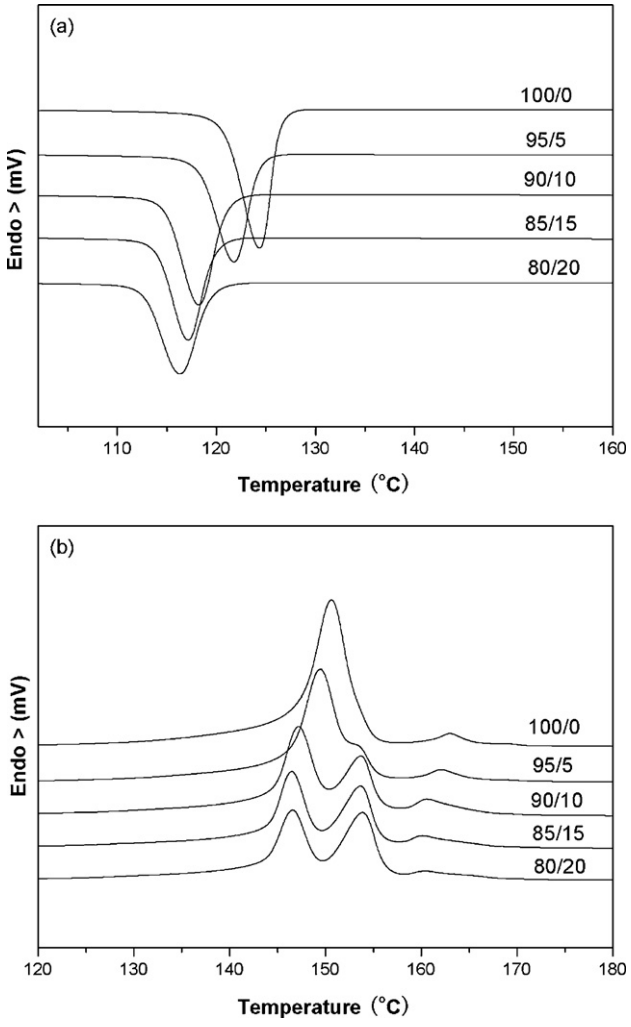

Fig. 1. Crystallization (a) and melting (b) curves of β-nucleated iPP/EVA-g-MA blend with various contents of EVA-g-MA.

2. Experimental

2.1. Materials

Isotactic polypropylene (iPP, HP500N) was homopolymer grade, supplied by CNOOC and Shell Petrochemicals Co., Ltd, MFI = 12 g/10 min (230 °C, 2.16 kg). Polyamide 6 (PA6, Grade M2800) has a relative viscosity of 2.83, supplied by Guangdong Xinhui Media Nylon Co., Ltd, MFI = 11 g/10 min (230 °C, 2.16 kg).

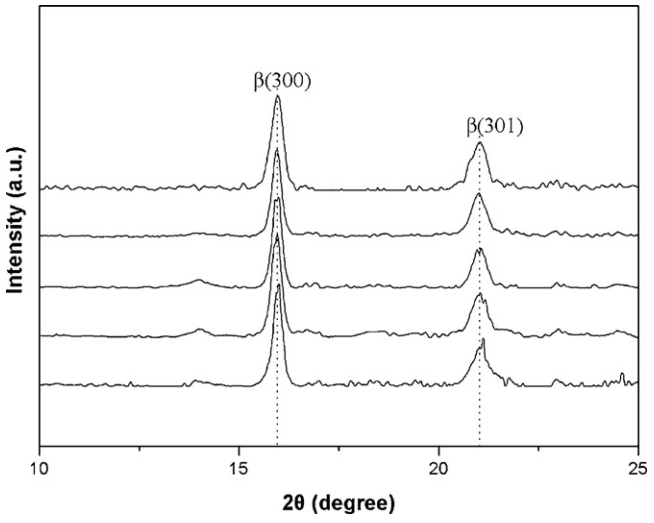

Fig. 2. XRD spectra of β-nucleated iPP/EVA-g-MA blend with various contents of EVA-g-MA.

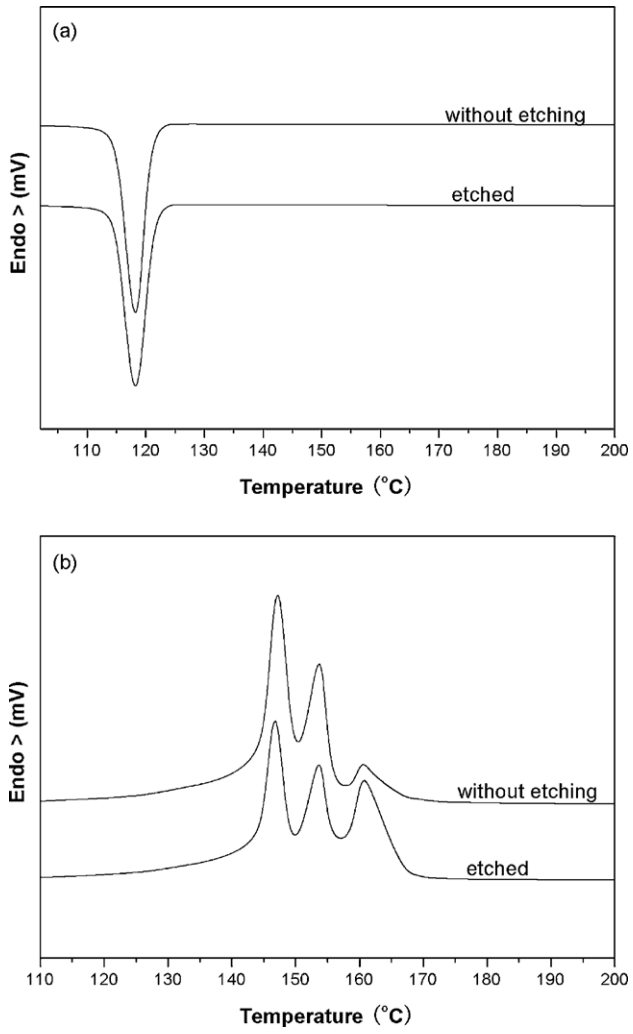

Fig. 3. Crystallization (a) and melting (b) curves of β-nucleated iPP/EVA-g-MA 90/10 blend and etched version with sulfuric acid.

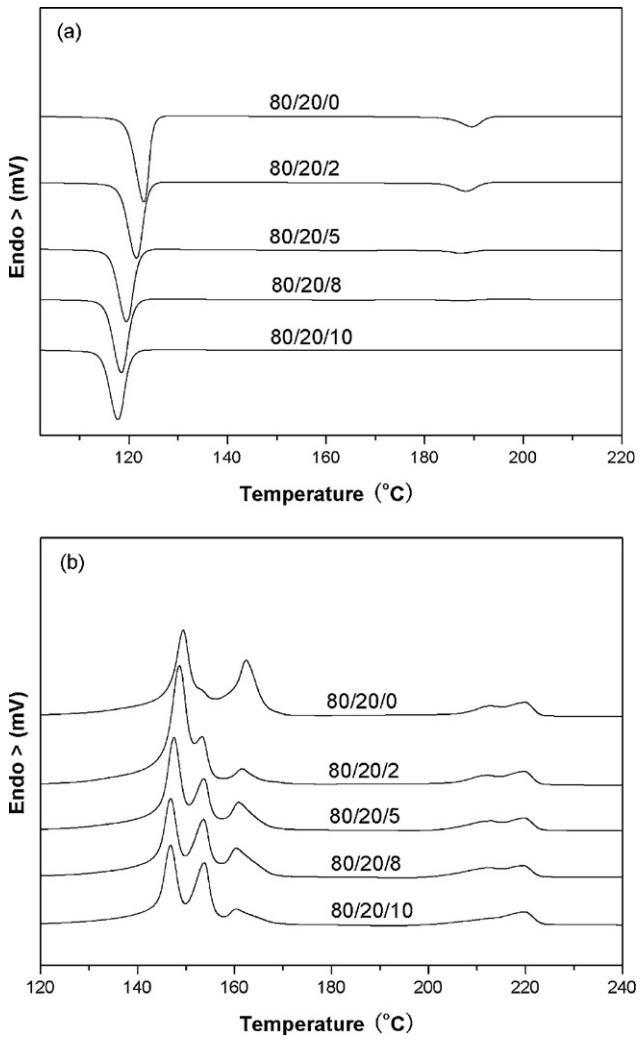

Fig. 4. Crystallization (a) and melting (b) curves of β-nucleated iPP/PA6 80/20 blend compatibilized with various contents of EVA-g-MA.

EVA-g-MA was commercial products, supplied by Guangzhou Lushan Chemical Materials Co., Ltd. The grafted content of MA was 1.0 wt.%, VA content 28%, $T_g = -28.8\,^{\circ}C$ (melting from −90 to 220 °C), $T_c^P = 52.2\,^{\circ}C$ (cooling from 220 °C to room temperature (−10 °C/min)), MFI = 2.46 g/10 min (190 °C, 2.160 kgf). A commercial grade of active nano-$CaCO_3$ with the particle diameter between 40 and 60 nm was obtained from Guangping Chemical Industry Limited Company, China, which had been pretreated with fatty acid in its production process. Aliphatic dicarboxylic acid was supplied by Shanghai Hongsheng Industry Co., Ltd, whose purity is 98%. A novel supported β-nucleating agent consisting of aliphatic dicarboxylic acid and nano-$CaCO_3$ (wt/wt, 1/50) was prepared in our lab [10,11]. Sulfuric acid (H_2SO_4), analytical reagent (AR), was obtained from Guangzhou Chemical Reagent Factory, whose content was 95–98 wt.%. Potassium carbonate (K_2CO_3), AR, was supplied by Tianjin Damao Chemical Reagent Factory.

2.2. Sample preparation

Before blending, all the materials were adequately dried in a vacuum oven at appropriate temperatures (PP at 80 °C, PA6 at 105 °C, EVA-g-MA at 60 °C and nano-$CaCO_3$ at 60 °C) for 12 h. 5 wt.% nano-$CaCO_3$ supported β-nucleating agents were added into iPP to prepare β-nucleated iPP on a twin-screw extruder at 180 °C with the screw rotation of 480 rpm and residue time of 40 s. Extrudates were cooled in a water bath and cut into pellets by a pelletizer.

The β-nucleated iPP/PA6 80/20 and the compatibilized version with EVA-g-MA blends were prepared using an internal mixer (Rheocord 300p, Germany) at 240 °C and 50 rpm, mixed for 8 min. In the same case, but the mixing temperature was changed to 180 °C for preparing β-nucleated iPP/EVA-g-MA blend. All the blends composed of various compositions were shown in Table 1.

Small thin pieces cut from β-nucleated iPP/EVA-g-MA and β-nucleated iPP/PA6 blends were dipped into sulfuric acid for 24 h to etch EVA-g-MA and PA6 component, respectively. Then the blend was washed with the potassium carbonate solution and large amount of distilled water in turn, at last, it was dried in a vacuum oven at 80 °C for 12 h for DSC measurements.

2.3. Differential scanning calorimeter

DSC measurements were made on a TA DSC Q10 differential scanning calorimeter (DSC), the temperature calibrated using pure indium in nitrogen atmosphere with heating rate of 10 °C/min. After calibration, the baseline is a line parallel to the *X*-axis with almost no positive or negative drift throughout the instrument's entire temperature range. The sample, about 5 mg for each, was heated to 260 °C with 10 °C/min, held there for 5 min, and then cooled to 100 °C with cooling rate of 10 °C/min. This controlled

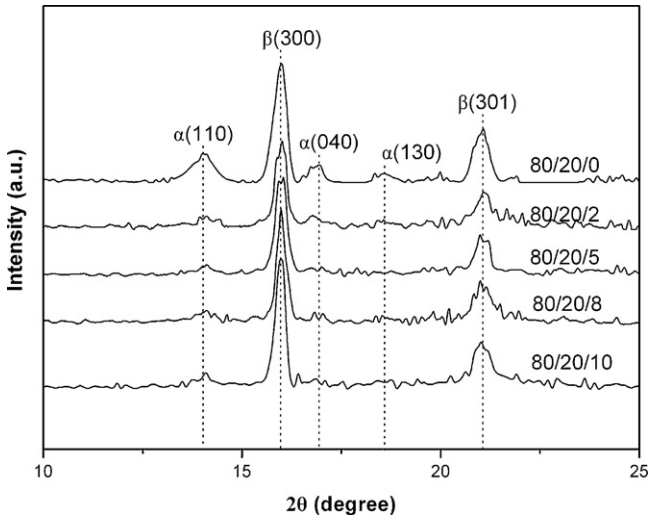

Fig. 5. XRD spectra of β-nucleated iPP/PA6 80/20 blend compatibilized with various contents of EVA-g-MA.

temperature prevents β–α transformation, so the polymorphic composition of the sample can be determined accurately for the melting curves [1,24]. The sample was reheated to 260 °C with the heating rate of 10 °C/min for melting behavior study. For the β-nucleated iPP/EVA-g-MA blend, the final heating temperature was designed at 220 °C.

2.4. Wide angle X-ray diffraction

The wide angle X-ray diffraction (WAXD) patterns of the samples were recorded at room temperature using a Rigaku D/Max 2200 unit equipped with Ni-filtered Cu K_α radiation in the reflection mode with a wavelength of 0.154 nm. For direct comparison, the specimens were prepared on TA DSC Q10 thermal system under the condition, where heated to designed temperature with 40 °C/min, held there for 5 min, and then cooled to 40 °C with cooling rate of 10 °C/min. The operating condition of the X-ray source was set at a voltage of 40 kV and a current of 30 mA in a range of $2\theta = 5–35°$ with a step scanning rate of 4°/min. The relative β-crystal content (K_β) was calculated according to the equation suggested by Turner-Jones et al. [30]:

$$K_\beta = \frac{I_{\beta 1}}{I_{\beta 1} + I_{\alpha 1} + I_{\alpha 2} + I_{\alpha 3}} \quad (1)$$

where $I_{\beta 1}, I_{\alpha 1}, I_{\alpha 2}, I_{\alpha 3}$ is the diffraction intensity of β (3 0 0), α (1 1 0), α (0 4 0) and α (1 3 0) planes, respectively.

2.5. Microscope

Specimens were examined using a JSM-6330F Field Emission Scanning Electron Microscope (SEM). The accelerating voltage was set at 10 kV. All SEM specimens were coated with platinum/palladium blend to avoid charging and thereby improving image quality. To obtain a survey of the phase structure, cryo-fractured surfaces of the blend obtained at liquid nitrogen temperature were examined.

3. Results and discussion

3.1. The effect of EVA-g-MA on β-nucleated iPP

Fig. 1 presents the crystallization and melting curves of β-nucleated iPP/EVA-g-MA blends with different contents of EVA-g-MA and the relative parameters are listed in Table 1. It can be observed that the intensity of crystallization peak and the crystallization temperature (T_c^p) decreases with increasing EVA-g-MA content for β-nucleated iPP/EVA-g-MA blends. The T_c^p of PP for neat β-nucleated iPP is 124.3 °C, but it decreased to 116.3 °C for β-nucleated iPP/EVA-g-MA blend containing 20 wt.% EVA-g-MA. The sole intensive melting peak of β-crystal at about 150 °C and a weak peak of α-crystal near to 160 °C are both observed for neat β-nucleated iPP (Fig. 1(b)). However, for the β-nucleated iPP/EVA-g-MA blends, another melting peak appears at round 155 °C and the original melting peak shifts to low temperature (near to 145 °C). Moreover, the intensity of melting peak at low temperature decreases but the one at high temperature increases with increasing EVA-g-MA content.

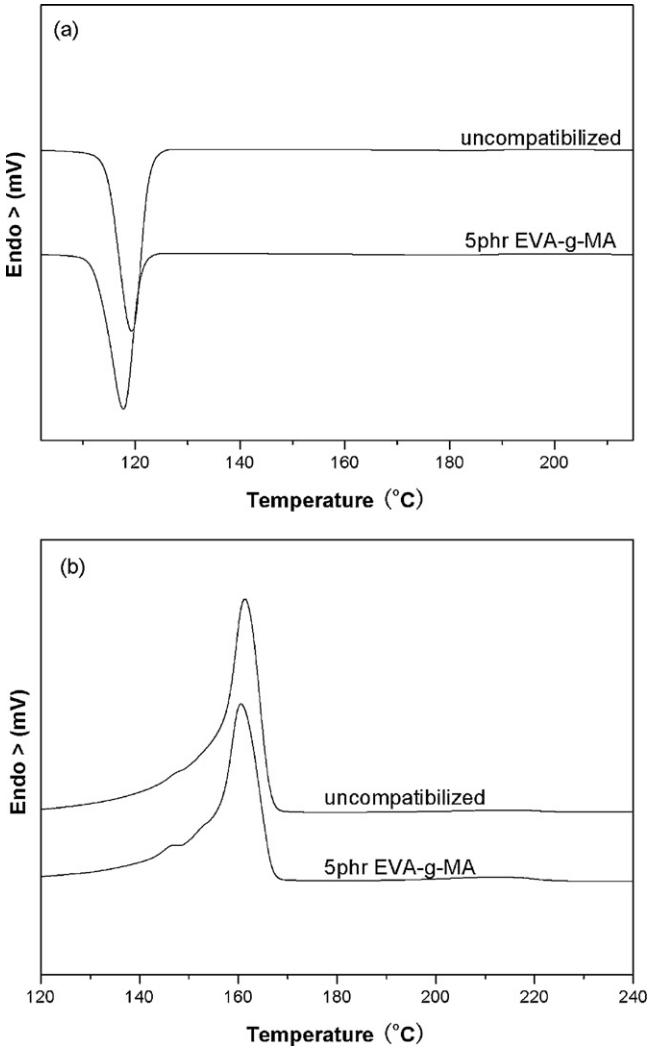

Fig. 6. Crystallization (a) and melting (b) curves of β-nucleated iPP/PA6 80/20 blend and compatibilized version with 5 phr EVA-g-MA etched with sulfuric acid.

The WAXD spectra of β-nucleated iPP/EVA-g-MA blends with various contents of EVA-g-MA are shown in Fig. 2. The intensities of diffraction peaks appearing at $2\theta = 16.1°$ and 21.3° are very strong, which is corresponded to the planes (3 0 0) and (3 0 1) of β-crystal [18,19], respectively. However, the diffraction peak relative to α-crystal was very weak or almost absent. The relative β-crystal content (K_β) for neat β-nucleated iPP and its blends (>95%) were listed in Table 1 according to Eq. (1), which was not obviously influenced by EVA-g-MA content.

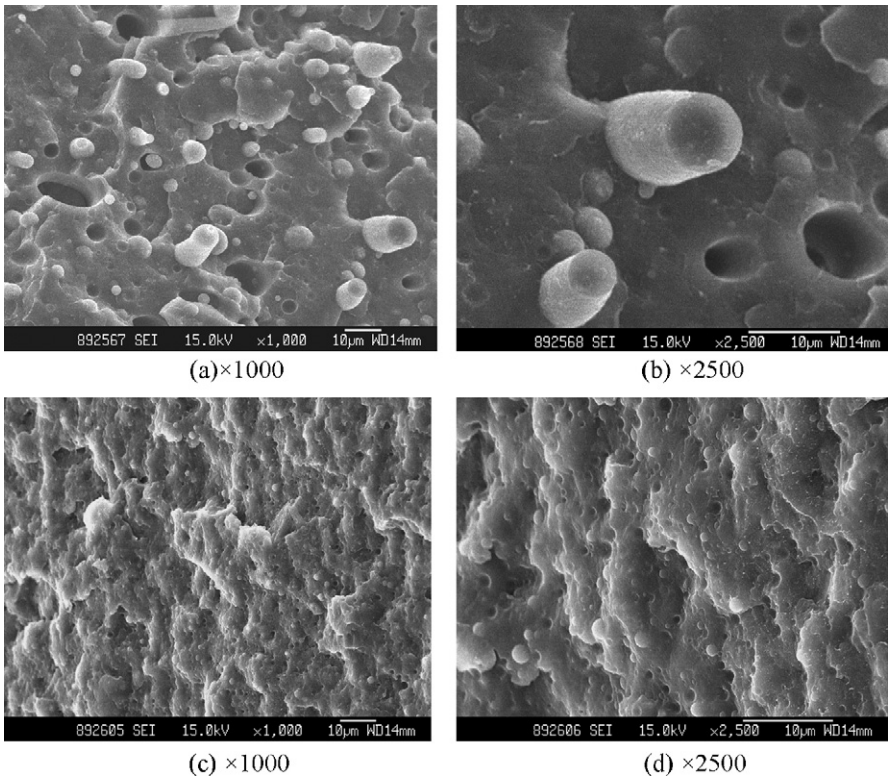

Fig. 7. SEM cryo-fractographs of β-nucleated iPP/PA6 blend uncompatibilized (a) ×1000, (b) ×2500 and compatibilized with 5 phr EVA-g-MA (c) ×1000, (d) ×2500.

Compared to the T_c^p of iPP for neat β-nucleated iPP, it shifts to low temperature for β-nucleated iPP/EVA-g-MA blend. It has been reported [31] that the backbone of EVA-g-MA containing the polar acetate group, is different from that of PP and considered immiscible with PP. The addition of EVA-g-MA hinders crystallization of iPP. What's more, the nucleating agent may transfer to the EVA-g-MA phase due to the polar interaction between them, which results in the decrease of its nucleation for iPP as well as the T_c^p of iPP. However, it almost makes no obvious differences that the β-crystal content for neat β-nucleated iPP and β-nucleated iPP/EVA-g-MA blends, which is suggested that the addition of EVA-g-MA has no pronounced effects on the β-nucleating ability of the supported β-nucleating agent, and a matrix of β-crystal was predominantly formed in the blends.

The blend was etched with sulfuric acid at room temperature for 24 h in order to prove the hypothesis that the β-nucleating agent may transfer to EVA-g-MA phase. Fig. 3 presents the crystallization and melting curves of β-nucleated iPP/EVA-g-MA 90/10 and its etched version. As is shown in Fig. 3, the T_c^p of iPP for the blend was independent of etching with sulfuric acid. However, the different melting behaviors were apparent between the blend and the etched one. Compared to the blend without etching, the intensity of β-crystal reduced and that of α-crystal increased for the blend etched with sulfuric acid. It has been observed that the etching with sulfuric acid has no effects on the β-crystal for neat β-nucleated iPP [27]. However, for the β-nucleated iPP/EVA-MA blend, the intensity of melting peak for β-crystal decreased obviously. It is attributed that parts of β-nucleating agent dispersed in EVA-g-MA phase was etched by sulfuric acid together with EVA-g-MA. Therefore, the efficiency of the β-nucleating agent decreased, which resulted in the decrease of the β-crystal content for the blend.

3.2. The effect of EVA-g-MA on β-nucleated iPP/PA6

The crystallization and melting curves of β-nucleated iPP/PA6 80/20 compatibilized with various contents of EVA-g-MA are shown in Fig. 4 and the relative parameters are also listed in Table 1. The T_c^p of iPP for β-nucleated iPP/PA6 blend compatibilized with EVA-g-MA shifts to low temperature, compared to that for the uncompatibilized one. Moreover, the intensity of the crystallization peak and the T_c^p of iPP decrease with increasing EVA-g-MA content in its compatibilized β-nucleated iPP/PA6 blend (Table 1). For example, the T_c^p of iPP decreased from 123.1 °C for β-nucleated iPP/PA6 blend to 117.8 °C for that compatibilized with 10 phr EVA-g-MA, which is similar with β-nucleated iPP/EVA-g-MA blend and the reason has been discussed above.

The crystallization peak of PA6 was apparent at around 190 °C for the uncompatibilized blend. However, for the one compatibilized with EVA-g-MA, the intensity of PA6 crystallization peak became weaker obviously and even disappeared with increasing EVA-g-MA content. It is suggested that the addition of EVA-g-MA increased the homogeneity of PA6 phase dispersion in the iPP matrix, with a reduction in the size of the domains of PA6 phase and resulted in the formation of EVA-g-PA copolymer in the interface between iPP and PA6, which also resulted in the reduction of the crystallinity of PA6 [32,33].

As is shown in Fig. 4(b), the melting behavior of the β-nucleated iPP/PA6 blend much depends on the content of EVA-g-MA. For the uncompatibilized blend, both the melting peak of β-crystal and α-crystal are presented at round 150 and 160 °C, respectively. However, for the blends compatibilized with EVA-g-MA, double-melting peaks of β-crystal can be observed and the intensity of α-crystal melting peak became obviously weaker. In addition, with increasing the EVA-g-MA content, the intensity of melting peak of β-crystal

at low temperature reduced but that at high temperature increased, which is similar to that of iPP/EVA-g-MA blend.

The WAXD spectra of β-nucleated iPP/PA6 blends compatibilized with different EVA-g-MA contents are presented in Fig. 5. For the uncompatibilized blend, it can be observed the reflection appeared at $2\theta = 14.3^\circ$, 16.8°, 18.6° and 16.1° corresponding to the planes (1 1 0), (0 4 0), (1 3 0) of α-crystal and the plane (3 0 0) of β-crystal, respectively. However, for the blend compatibilized with EVA-g-MA, the intensity of the diffraction peak of β-crystal increased and that of α-crystal decreased or even disappeared with increasing the EVA-g-MA content in the β-nucleated iPP/PA6 blends. Moreover, the relative β-crystal content (K_β) examined according to the Eq.1 was listed in Table 1. The β-crystal content for the blend compatibilized with 10 phr EVA-g-MA increased to 96%, compared with 66% for the uncompatibilized β-nucleated iPP/PA6 blend.

It can be suggested that the β-nucleating agent in iPP might move to PA6 phase and/or the interface between iPP and PA6 due to the interaction between the polar groups of β-nucleating agent and the polar groups of PA6 for the blend without compatibilizer in the process of blending at high temperature. This interaction decreased the concentration of β-nucleating agent in iPP matrix and resulted in the decrease in the nucleation effect of β-nucleating agent. On the other hand, there is a competition between the selective encapsulation of the nucleating agents and the α-nucleating effect of PA6 in β-nucleated iPP/PA6 blends, which can also hinder the formation of β-crystal [26–28]. On the contrary, the addition of EVA-g-MA is benefit for the formation of the matrix rich in β-crystal, which is attributed to that the β-nucleating agent is prior to distribute into EVA-g-MA phase due to its stronger polarity than PA6 but its nucleation efficiency would not reduce according to the results of β-nucleated iPP/EVA-g-MA blend. Moreover, the addition of EVA-g-MA increased the homogeneity of PA6 phase dispersed in the iPP matrix with a reduction in the size of the domains due to the compatibilization of EVA-g-MA, which resulted in the reduce of the interaction between the β-nucleating agent and PA6 and no effects on its nucleation efficiency for iPP. In conclusion, EVA-g-MA is benefit for the formation the matrix rich in β-crystal for β-nucleated iPP/PA6 blends.

Fig. 6 illustrates the crystallization and melting curves of β-nucleated iPP/PA6 80/20 blend and compatibilized version with 5 phr EVA-g-MA etched with sulfuric acid for 24 h at room temperature. As shown in Fig. 6, the crystallization and melting peaks of PA6 were both absent, which is indicated that the PA6 phase was almost completely etched by sulfuric acid in β-nucleated iPP/PA6 blends. What's more, the intensity of β-crystal melting peak is very weak or almost disappeared (Fig. 6(b)), which is suggested that the β-nucleating agent mainly dispersed in PA6 or EVA-g-MA and/or the interface between them. As a result, the β-nucleating agent was etched and the matrix rich in α-crystal was formed in β-nucleated iPP/PA6 blend.

3.3. Phase morphology

It was previously reported that the blend of iPP/PA6 is immiscible because of the obvious differences in their polarity [33]. Fig. 7 presents the SEM images of the β-nucleated iPP/PA6 80/20 and compatibilized version with 5 phr EVA-g-MA. It can bee clearly seen that the size of PA6 particle is large and poor bonded with iPP for the uncompatibilized β-nucleated iPP/PA6 blend, from Fig. 7(a) and (b) with various magnification times. The β-nucleating agent was reunited on the surface of PA6 due to the polar interaction between them. However, for the blend compatibilized with EVA-g-MA (Fig. 7(c) and (d)), the size of PA6 particle obviously reduced and homogeneously distributed in iPP phase. Moreover, the β-nucleating agent was well dispersed in iPP phase and facilitated the formation of β-crystal.

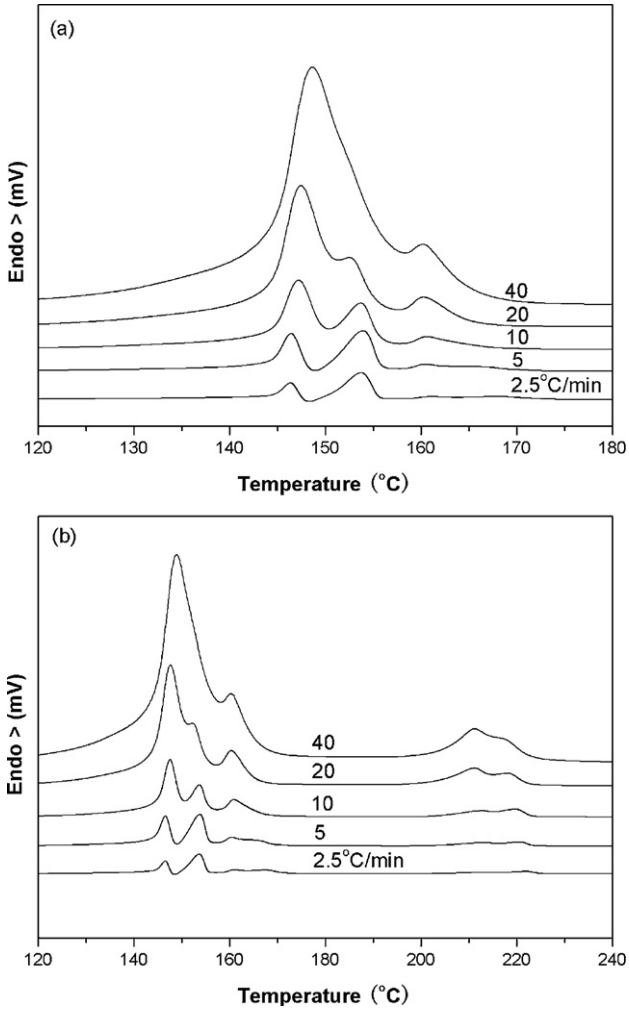

Fig. 8. Melting curves of β-nucleated iPP/EVA-g-MA 90/10 (a) and β-nucleated iPP/PA6 80/20 blend compatibilized with 5 phr EVA-g-MA (b) with various heating rates.

3.4. The explanation for the double-melting peaks of β-crystal in the blend

It can be observed the double-melting peaks of β-crystal from Figs. 1(b) and 4(b) for β-iPP/EVA-g-MA and β-iPP/PA6 blend compatibilized with EVA-g-MA. In order to find out the formation mechanism of the double-melting peaks, β-nucleated iPP/EVA-g-MA 90/10 and β-nucleated iPP/PA6 80/20 blend compatibilized with 5 phr EVA-g-MA were heated up to 260 °C and held there for 5 min, then cooled to 100 °C with the same cooling rate of 10 °C/min before recorded the melting curves (Fig. 8) with different heating rates. As shown in Fig. 8, double-melting peaks of β-crystal can be observed obviously when the heating rate is lower than 20 °C/min. The intensity of low-temperature melting peak increased and that of high-temperature melting peak decreased with increasing the heating rates.

This effect is typically associated with melting followed by re-crystallization into more stable crystals and re-melting of the re-crystallized material at higher temperature. The addition of EVA-g-MA reduced the T_c^p of β-iPP and resulted in the formation of non-perfect β-crystals, which was easy to re-crystallize to form more perfect crystals during the heating process. The non-perfect

crystals had enough times to re-crystallize to more perfect ones at lower heating rates and the melting temperature was also higher. However, at higher heating rates, the process of re-crystallization (and thus also re-melting) is hindered due to short times, resulting in only one low-temperature melting peak. In a word, the original β-crystals melt and re-crystallize into more perfect ones.

4. Conclusions

On the basis of our experimental results, the addition of EVA-g-MA reduced the crystallization temperature of β-nucleated iPP due to its hindering iPP crystallization. However, it has no pronounced effects on β-crystal content for β-nucleated iPP/EVA-g-MA blends. On the other hand, PA6 decreased the β-crystal content of β-nucleated iPP. However, the addition of EVA-g-MA is benefit for the formation of a matrix rich β-crystal for β-nucleated iPP/PA6 blend although the addition of EVA-g-MA decreased the crystallization temperature of iPP in the blend. The efficiency of β-nucleating agent is much relative to its dispersion in various phases, which was supported by the etching experiment and SEM images. Double β-crystal melting peaks can be observed for both β-nucleated iPP/EVA-g-MA and compatibilized β-nucleated iPP/PA6 blend, which is relative to the original β-crystals melting and re-crystallization into more perfect ones.

Acknowledgements

The author would like to thank the support from China Scholarship Council. The work was supported by Natural Science Foundation of China (Grant No. 50873115) and Doctoral Fund of Ministry of Education of China.

References

[1] J. Varga, β-Modification of isotactic polypropylene: preparation, structure, processing, properties, and application, J. Macromol. Sci. Phys. 41 (2002) 1121–1171.
[2] C. Grein, C.J.G. Plummer, H.H. Kausch, Y. Germain, P. Beguelin, Influence of β-nucleation on the mechanical properties of isotactic polypropylene and rubber modified isotactic polypropylene, Polymer 43 (2002) 3279–3293.
[3] F. Luo, C.Z. Geng, K. Wang, H. Deng, F. Chen, Q. Fu, B. Na, New understanding in tuning toughness of β-polypropylene: the role of β-nucleated crystalline morphology, Macromolecules 42 (2009) 9325–9331.
[4] Y.H. Chen, G.J. Zhong, Y. Wang, Z.M. Li, L.B. Li, Unusual tuning of mechanical properties of isotactic polypropylene using counteraction of shear flow and beta-nucleating agent on β-form nucleation, Macromolecules 42 (2009) 4343–4348.
[5] H. Zhu, B. Monrabal, C.C. Han, D. Wang, Phase structure and crystallization behavior of polypropylene in-reactor alloys: insights from both inter- and intramolecular compositional heterogeneity, Macromolecules 41 (2008) 826–833.
[6] H.B. Chen, J. Karger-Kocsis, J.S. Wu, J. Varga, Fracture toughness of α- and β-phase polypropylene homopolymers and random- and block-copolymers, Polymer 43 (2002) 6505–6514.
[7] M. Raab, J. Scudla, J. Kolarik, The effect of specific nucleation on tensile mechanical behaviour of isotactic polypropylene, Eur. Polym. J. 40 (2004) 1317–1323.
[8] A. Tedesco, P.F. Krey, R.V. Barbosa, R.S. Mauler, Effect of the type of nylon chain-end on the compatibilization of PP/PP-GMA/nylon 6 blends, Polym. Int. 51 (2002) 105–110.
[9] Q.F. Yi, X.F. Wen, J.Y. Dong, C.C. Han, A novel effective way of comprising a β-nucleating agent in isotactic polypropylene (i-PP): polymerized dispersion and polymer characterization, Polymer 49 (2008) 5053–5063.
[10] Z.S. Zhang, Y.J. Tao, Z.G. Yang, K.C. Mai, Preparation and characteristics of nano-$CaCO_3$ supported β-nucleating agent of polypropylene, Eur. Polym. J. 44 (2008) 1955–1961.
[11] Z.S. Zhang, C.G. Wang, Z.G. Yang, C.Y. Chen, K.C. Mai, Crystallization behavior and melting characteristics of PP nucleated by a novel supported β-nucleating agent, Polymer 49 (2008) 5137–5145.
[12] X.L. Sun, H.H. Li, X.Q. Zhang, D.J. Wang, J.M. Schultz, S. Yan, Effect of matrix molecular mass on the crystallization of β-form isotactic polypropylene around an oriented polypropylene fiber, Macromolecules 43 (2010) 561–564.
[13] N. Mohmeyer, H.W. Schmidt, P.M. Kristiansen, V. Altstadt, Influence of chemical structure and solubility of bisamide additives on the nucleation of isotactic polypropylene and the improvement of its charge storage properties, Macromolecules 39 (2006) 5760–5767.
[14] P.W. Zhu, J. Tung, A. Phillips, G. Edward, Morphological development of oriented isotactic polypropylene in the presence of a nucleating agent, Macromolecules 39 (2006) 1821–1831.
[15] A.J. Lovinger, Microstructure and unit-cell orientation in alpha-polypropylene, J. Polym. Sci. B: Polym. Phys. 21 (1983) 97–110.
[16] S.V. Meille, D.R. Ferro, S. Bruckner, A.J. Lovinger, F.J. Padden, Structure of β-isotactic polypropylene – a long-standing structural puzzle, Macromolecules 27 (1994) 2615–2622.
[17] J. Moitzi, P. Skalicky, Shear-induced crystallization of isotactic polypropylene melts – isothermal waxs experiments with synchrotron-radiation, Polymer 34 (1993) 3168–3172.
[18] R.H. Somani, B.S. Hsiao, A. Nogales, H. Fruitwala, S. Srinivas, A.H. Tsou, Structure development during shear flow induced crystallization of i-PP: in situ wide-angle X-ray diffraction study, Macromolecules 34 (2001) 5902–5909.
[19] R.H. Somani, B.S. Hsiao, A. Nogales, S. Srinivas, A.H. Tsou, I. Sics, F.J. Balta-Calleja, T.A. Ezquerra, Structure development during shear flow-induced crystallization of i-PP: in-situ small-angle X-ray scattering study, Macromolecules 33 (2000) 9385–9394.
[20] H. Huo, S.C. Jiang, L.J. An, J.C. Feng, Influence of shear on crystallization behavior of the β-phase in isotactic polypropylene with β-nucleating agent, Macromolecules 37 (2004) 2478–2483.
[21] M. Feng, F.L. Gong, C.G. Zhao, G.M. Chen, S.M. Zhang, M.S. Yang, C.C. Han, The β-crystalline form of isotactic polypropylene in blends of isotactic polypropylene and polyamide-6/clay nanocomposites, J. Polym. Sci. B: Polym. Phys. 42 (2004) 3428–3438.
[22] J. Varga, β-Modification of polypropylene and its two component systems, J. Therm. Anal. 35 (1989) 1891–1912.
[23] G.Y. Shi, Recent Studies on β-Crystalline Form of Isotactic Polypropylene, Springer Verlag, Berlin, 1994.
[24] A. Menyhárd, J. Varga, The effect of compatibilizers on the crystallisation, melting and polymorphic composition of β-nucleated isotactic polypropylene and polyamide 6 blends, Eur. Polym. J. 42 (2006) 3257–3268.
[25] Y.J. Tao, Y.X. Pan, Z.S. Zhang, K.C. Mai, Non-isothermal crystallization, melting behavior and polymorphism of polypropylene in β-nucleated polypropylene/recycled poly(ethylene terephthalate) blends, Eur. Polym. J. 44 (2008) 1165–1174.
[26] Z.G. Yang, C.Y. Chen, D.W. Liang, Z.S. Zhang, K.C. Mai, Melting characteristic and beta-crystal content of β-nucleated polypropylene/polyamide 6 alloys prepared using different compounding methods, Polym. Int. 58 (2009) 1366–1372.
[27] Z.G. Yang, Z.S. Zhang, Y.J. Tao, K.C. Mai, Effects of polyamide 6 on the crystallization and melting behavior of β-nucleated polypropylene, Eur. Polym. J. 44 (2008) 3754–3763.
[28] Z.G. Yang, Z.S. Zhang, Y.J. Tao, K.C. Mai, Preparation, crystallization behavior, and melting characteristics of β-nucleated isotactic polypropylene blends with polyamide 6, J. Appl. Polym. Sci. 112 (2009) 1–8.
[29] A. Menyhárd, J. Varga, A. Liber, G. Belina, Polymer blends based on the β-modification of polypropylene, Eur. Polym. J. 41 (2005) 669–677.
[30] A. Turner-Jones, J.M. Aizlewood, D.R. Beckett, Crystalline forms of isotactic polypropylene, Makromol. Chem. 75 (1964) 134–158.
[31] B.M. Huerta-Martinez, E. Ramirez-Vargas, F.J. Medellin-Rodriguez, R.C. Garcia, Compatibility mechanisms between EVA and complex impact heterophasic PP–EPx copolymers as a function of EP content, Eur. Polym. J. 41 (2005) 519–525.
[32] B. Ohlsson, H. Hassander, B. Tornell, Improved compatibility between polyamide and polypropylene by the use of maleic anhydride grafted SEBS, Polymer 39 (1998) 6705–6714.
[33] W.S. Chow, A. Abu Bakar, Z.A.M. Ishak, J. Karger-Kocsis, U.S. Ishiaku, Effect of maleic anhydride-grafted ethylene-propylene rubber on the mechanical, rheological and morphological properties of organoclay reinforced polyamide 6/polypropylene nanocomposites, Eur. Polym. J. 41 (2005) 687–696.